Sensing and Bio-Sensing Research 35 (2022) 100469

Contents lists available at ScienceDirect

Sensing and Bio-Sensing Research

journal homepage: www.elsevier.com/locate/sbsr

Performance analysis of alcohols sensing with optical sensor procedure using circular photonic crystal fiber (C-PCF) in the terahertz regime

Md. Selim Hossain [a], Nazmul Hussain [b], Zakir Hossain [c], Md. Sakib Zaman [d], Md. Navid Hasan Rangon [d], Md. Abdullah-Al-Shafi [e], Shuvo Sen [f,*], Mir Mohammad Azad [g]

[a] Department of Computing and Information System (CIS), Daffodil International University, Dhaka, Bangladesh
[b] Department of Information and Communication Engineering, Bangladesh Army University of Engineering and Technology, Qadirabad Cantonment, Natore 6431, Bangladesh.
[c] Department of Computer Science and Engineering, Asian University of Bangladesh, Dhaka, Bangladesh
[d] Department of Physics, Mawlana Bhashani Science and Technology University, Santosh, Tangail 1902, Bangladesh
[e] Institute of Information Technology, University of Dhaka, Dhaka, Bangladesh
[f] Department of Information and Communication Technology (ICT), Mawlana Bhashani Science and Technology University, Santosh, Tangail 1902, Bangladesh
[g] Department of Computer Science and Engineering, Hamdard University, Bangladesh

ARTICLE INFO

Keywords:
C-PCF
THz wave
PCF
CL
RS
Effective area
Total power fraction

ABSTRACT

In this study, a TOPAS-based optical sensor for detecting alcohols in drinks and liquids, made of circular air holes (CAH) in the cladding and a hexahedron core is suggested here. In addition, COMSOL Multiphysics program for development and analysis of the sensing qualities of a PCF-based sensor using finite element technical as a solution. In the THz frequency band, the described C-PCF structure has an exceptionally high relative sensitivity of 86.60%, 88.70%, and 84.71%, and low confinement losses (CL_s) are 5.75×10^{-08}, 6.11×10^{-08} dB/m and 5.70×10^{-08} dB/m for three alcohols such as Ethanol ($n = 1.354$), Butanol ($n = 1.399$), and Propanol ($n = 1.387$), respectively at monitoring region of 1 THz. Alcohol is widely used in both the food and beverage sectors and chemical operations. The detection methods of alcohol thus must be accurate, accurate, and reliable. This content modeling and analysis in the terahertz frequency range is a novel TOPAS-based photonic crystal fiber (C-PCF). Moreover, the total power fraction and effective area are also determined in the terahertz frequency range. Due to its excellent waveguiding characteristics, this suggested sensor has the potential to be employed in alcohols detection as well as polarization preserving terahertz wave applications.

1. Introduction

In recent decades, considerable endeavors have been made to develop photonic crystal fibers and to investigate their optical characteristics. The application field of fiber optic applications in the fields of optical feats is not just confined to telecommunications but, because of their optical properties, has shown tremendous potential in non-linear optics, in fiber lenses, in noninvasive medical imaging [1]. PCF has become prominent in THz applications for chemical sensing. The main reason of significant interest here is that it is possible to adjust the sensing properties by altering its geometrical parameters. Hollow-core PCF includes a higher volume of analysis within the core area than the porous core, which enhances light-to-matter interaction with enormous sensing possibilities. Alcohols are an intoxicant that may cause coma and death and can cause addiction in various drinks [2–4]. So, alcohols in drinks are therefore very important to identify.

Recently, several researchers have created various forms of PCF geometries in liquid samples to detect alcoholic or other chemicals substances. On the other hand, every researcher has used to many background materials such as ZEONEX, TOPAS to reduce the losses in their PCF structure [5–9]. The hybrid PCF was created by S. Asaduzzaman et al. [10] and the sensitivity to Ethanol recorded in this design was 49.17%. As sensors for low-loss and enhanced sensitive liquid sensing, Arif et al. [11] suggested hexagonal constructed PCF. Arif et al. proposed S. Asaduzzaman et al. suggested design gave them more sensitivity. With this in mind, the sensitivity of J. Sultana et al. [12] is increased by a ZEONEX grounded Ethanol sensing where 68.87% sensitivity with 7.79×10^{-12} cm^{-1} CL at 1 THz frequency had been found. Advanced, B. K.

* Corresponding author.
E-mail address: shuvombstu.it12009@gmail.com (S. Sen).

https://doi.org/10.1016/j.sbsr.2021.100469
Received 25 September 2021; Received in revised form 3 December 2021; Accepted 14 December 2021
Available online 17 December 2021

Paul et al. [13] planned a CAH based PCF with 64.19% Relative Sensitivity (RS) and CL of 2.07 × 10^{-5} dB/m is achieved for 1.48 μm. H. Ademgil et al. [14] suggested a PCF-based sensor for low-containment liquid analyte detection applications. Only 26% of sensitivity was attained with the suggested PCF. By using octagonal PCF K. Ahmed et al. [15] had obtained RS of 57% and a high CL. In view of the impacts of alcoholic drinks, we introduced a better photonic THz-based crystal fiber sensor in liquid samples for the detection of alcohols which is above a number of current literature designs [10–15].

We have proposed the alcohol PCF sensor with much better results in relative sensitivity of 86.50%, 88.35% and 84.71% of three 1-THz alcohols such as Ethanol (n = 1.354), Butanol (n = 1.399), and Propanol (n = 1.387), respectively. In addition, the lower confinement losses are 5.75 × 10^{-08}, 6.11 × 10^{-08} dB/m and 5.70 × 10^{-08} dB/m for three chemicals such as Ethanol (n = 1.354), Butanol (n = 1.399), and Propanol (n = 1.387), respectively at monitoring region of 1 THz. Not only this, our proposed structure of C-PCF also defines a higher relative sensitivity of 86% in industrial and alcohol sensing sector than those found previously in the articles [23–29].

2. Design methodology of the proposed sensor

Fig. 1 shows the cross-sectional view of the proposed sensor and the enlargement of the core region such as (a) Circular cladding area (b) Hexahedron core area. The pitch and diameter of the cladding surface are noted here by A_1 and d_1, and A_c, d_c by the Hexahedron's core surface is the pitch and diameter. In the hexahedron core area, the first layer of 6 circular air holes contains a 20° along with 60° angular differences and the second layer of 6 circular air holes contain a 20°, 80°, 120°, 180°, 240°, 300°. A perfectly matched (PML) layer, 10% of the total fiber, is utilized to safeguard the atmosphere. Due to its low material absorption loss, consistent reflection index in a broad range of frequencies, we picked TOPAS as backdrop material in our design proposal [10,11]. The optimum constraints of each cladding diameter 285 μm, cladding of each 3pitch 80 μm, core diameter d_c = 64 μm and core pitch A_c = 68 μm.

In Fig. 2, the light laser is passed through the analytic C-PCF core and the optical spectrum analyzer (OSA) will provide data to the computer to analyze the optical properties like effective area, RS, power fraction, CL, and effective mode index of the injected alcohols. Then the computer will represent data numerically and graphically procedure.

3. Mathematical analysis

The area covered by light intensity interaction with subjects can be quantified using the phrase effective area. For laser and communication devices a more effective area is enough whereas for nonlinear effects a lower modal EA is suitable [17]. It is distinguishable by [18]

$$A_{effective} = \frac{\left[\int I(r)rdr\right]^2}{\left[\int I^2(r)dr\right]^2} \quad (1)$$

Where, E_{eff} is the effective area and $I(r) = |E_t|^2$ is the cross-sectional electric field intensity.

For PCF, the power fraction can be determined by determining the amount of power or energy flowing through the photonic fiber structure, and by calculating this fraction. Thus, $\boldsymbol{P}$ is determined through the subsequent calculation of the PCF power fraction [19].

$$\boldsymbol{P} = \frac{\int_i S_z dA}{\int_{all} S_z dA} \quad (2)$$

When the numbering part of the calculation reveals the area of our interest such as core, cladding or air hole. In addition, the integral denominator shows the overall cross-sectional area of the PCF.

In describing the optical characteristics of PCF structure CL also consider as another important parameter. Not only that, PCF fibers display higher RS at lower CL. The following equation defines the CL L_c [20].

$$L_c = 8.686 \times K_0\, Im\left[n_{eff}\right]\ (dB/m) \quad (3)$$

Here, $k_0 = (f/c)$ where, f represents frequency and c represents speed of the photon. On the other hand, $I_m(n_{eff})$ = imaginary part of effective mode index.

From the Beer-Lambert Law we know that the photonic crystal fiber sensor completely relies on the light intensity of the matter interface [21],

$$I(f) = I_0(f)\, exp.[-r\alpha_m l_c] \quad (4)$$

Where I(f), before the analysis, the absorption factor, the αm factor and the channel extent of the illumination are shown, I_c defined I0 (f). Furthermore, f and r are respectively fiber frequency and RS.

An important parameter of absorbance (A) and the passed I0 light for

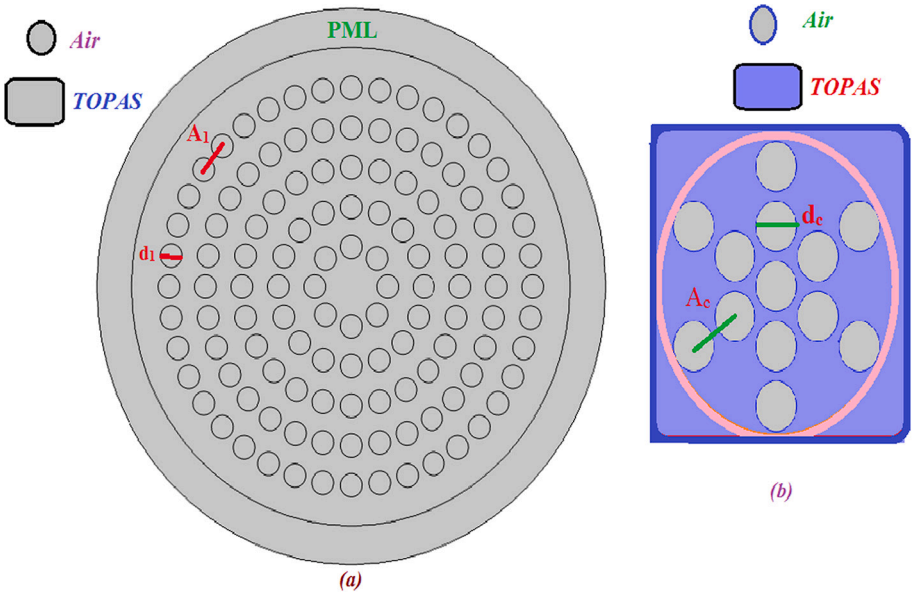

Fig. 1. C-PCF fiber structure with (a) Circular cladding region and (b) Hexahedron core region.

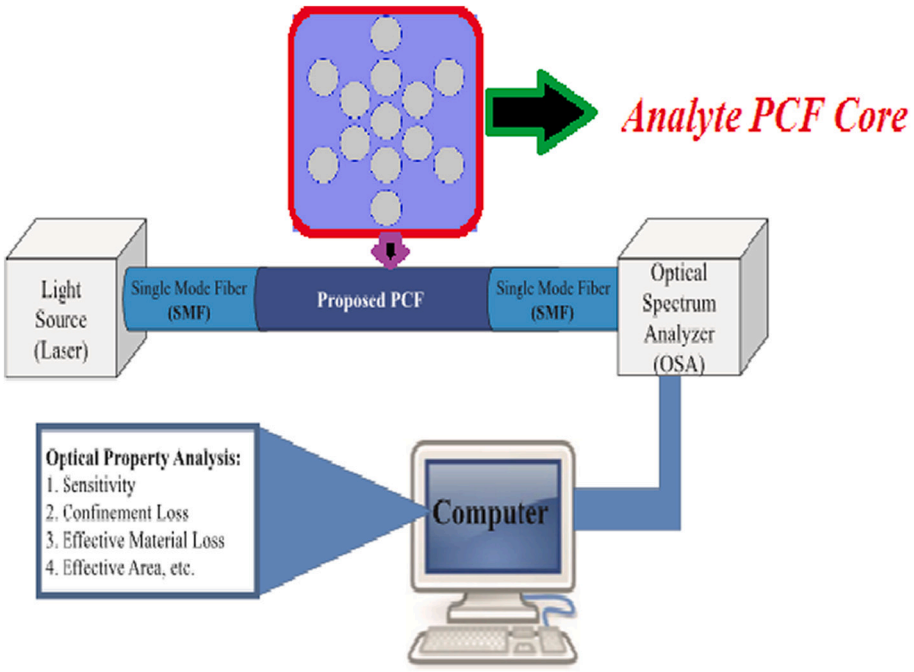

Fig. 2. Representation of working procedure of the proposed C-PCF model [16].

the analyzers are explained to explain the intensity of the photon (I).

$$A = log\left(\frac{I}{I_o}\right) = -r\alpha_m l_c, \tag{5}$$

It is worth mentioned that the RS of photonic crystal sensor is most import to check. The RS of PCF is determined by [22].

$$R = \frac{n_r}{n_{eff}} \times E \tag{6}$$

In this case n_r is the index refractive and n_{eff}, the mode index effective. In addition, by the following equation the absolute sum of the interface of light matter is estimated:

$$E = \frac{\int_{sample} R_e\left(E_x H_y - E_x H_y\right) dxdy}{\int_{total} R_e\left(E_x H_y - E_x H_y\right)\, dxdy} \times 100\% \tag{7}$$

Where the x, y element electric fields are defined by Ex and Ey each and where Hx and Hy are defined by their respective magnetic fields.

4. Output analysis and discussion

Result Analysis and Discussions: The COMSOL software 4.2, which calculates all numerical, analyzes and the frequency range from 0.80 to 3.0 THz, calculates them. Fig. 3 shows polarization of the mode of x and y optical field distributions at 1 THz. Moreover, we have found maximum relative sensitivity by this x and y optical mode and include the measurement of right side scale at the 1 THz region to detect the alcohols easily. Due to the containment of light, the susceptibility of both x and y polarizing of C-PCF design is increased. The separate light intensity for separate polarizations is distributed through the fibers and the loss of leakage, susceptibility, and other characteristics of the optical filament responsiveness are therefore largely changed. Likewise, some other variations for another change to a large extend. Similarly, some other variations for a different change of parameters are illustrated in

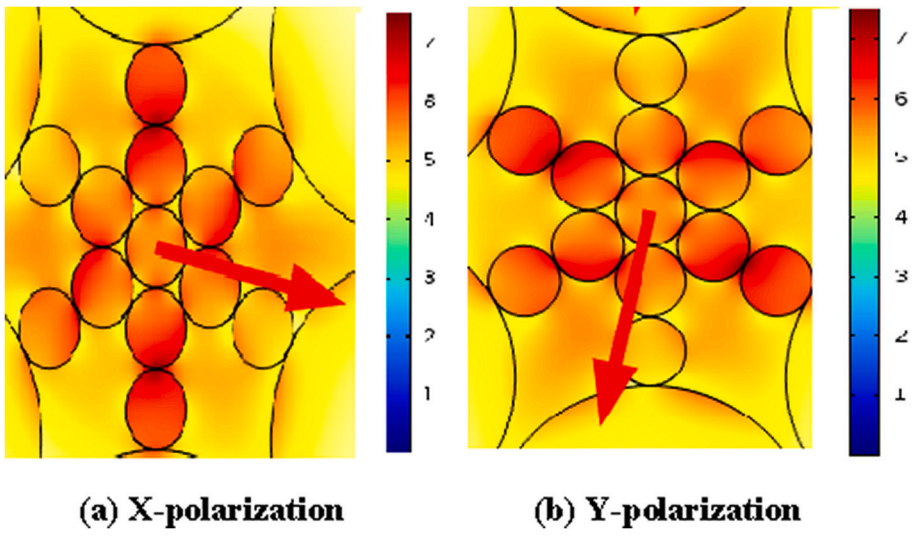

Fig. 3. Mode field distributions for (a) **X** -polarization and (b) **Y**-polarization.

Figs. 4 to 12.

In Fig. 4, the RS of the proposed C-PCF fiber is displayed together with the frequency of optimum parameters. In this figure, RS has been gradually decreased by a frequency increase (THz) of 0.8 THz to 1.2 THz and RS has been decreased gradually of 1.2 THz to 3 THz. The figure also reveals the maximum RS of Ethanol at a frequency of around 1 THz is 86.60% Ethanol, Butanol is 88.70%, and roughly 84.71% is Propanol. At this 1 THz region, we have found the maximum relative sensitivity. The lower relativity is measured by about 68% Ethanol, 70% Butanol and approximately 66% Propanol, with a 3 THz operating rate. Here, the optimum constraints are cladding diameter is 285 μm, cladding pitch is 380 μm, core diameter $d_c = 64$ μm and core pitch $A_c = 68$ μm.

Fig. 5 shows the link between the RS and the intended C-PCF frequency, with 3% more or less optimum parameters than the original core and cladding of the air holes for both the polarization. In the lower frequency range of the THz band, RS of 0.8–1.2 THz is also shown. The relative sensitiveness similarly declines, with the rise in frequency in the THz range, much resembling exponential behavior.

The RS for ethanol, butanol and propanol, for the purposes of Fig. 4 are 87.20%, 89.40%, and 85.30% for the 1 THz section, the RS for increased (+3%) parameters for five layers diameter of 293.55 μm and the five coat pitches of $A_1 = A_2 = A_3 = A_4 = A_5 = 391.40$ μm, the core pitch of $A_c = 70.04$ μm and core diameter $d_c = 64.92$ μm. Further RS is 85.10%, 87.30%, and 83.15% at ethanol, butanol and propanol for decreasing strands (−3%) at a controlling region of 1 THz, Here, the optimum parameters of 5 layers cladding diameters (individually) 276.45 μm and 5 layers cladding pitch is 368.60 μm, two layer with core diameter (d_c) = 62.08 μm, two layer core pitch $A_c = 65.96$ μm.

Fig. 6 discloses the effective area vs frequency for optical fiber parameters of the designed C-PCF fiber. It is seen that the effective area of C-PCF fiber almost exponentially decreases with the increases of frequency from 0.5 THz to 3 THz range. Moreover, the effective area for Ethanol is 1.36×10^{-7} m^2, for Butanol is 1.43×10^{-7} m^2 and 1.47×10^{-7} m^2 for Propanol at 1 THz. At this 1 THz area, this C-PCF fiber shows maximum relative sensitivity. Here, the optimum constraints are cladding diameter 285 μm, cladding pitch 380 μm, core diameter $d_c = 64$ μm and core pitch $A_c = 68$ μm.

Fig. 7 shows an optimum containment loss-in-frequency relationship between the designed C-PCF fiber. In the figure we see that the loss of containment decreases because of the increase of the THz band functional frequency. We also note that containment loss is constant between

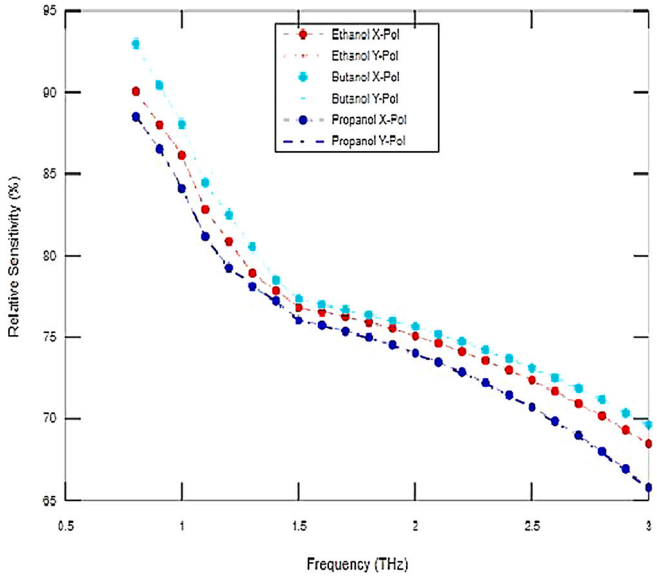

Fig. 4. RS versus frequency for Ethanol, Butanol and Propanol.

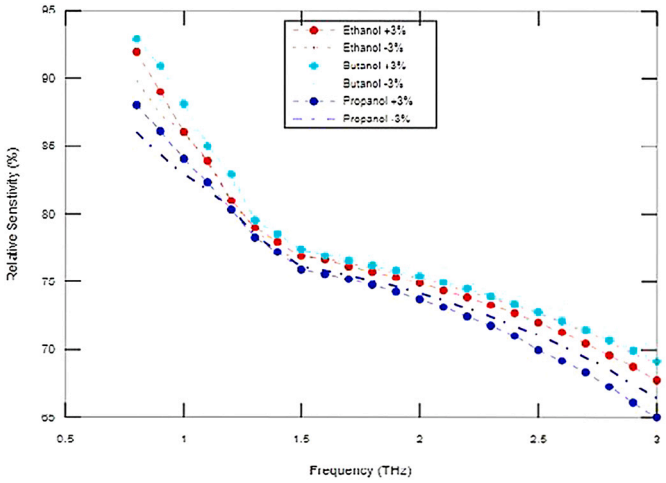

Fig. 5. RS versus frequency for Ethanol, Butanol and Propanol along with ±3% variations of core diameter.

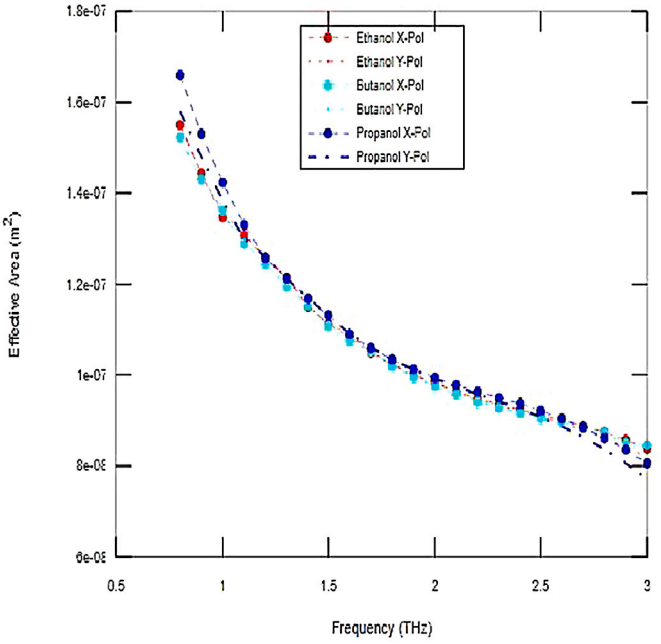

Fig. 6. Effective area versus frequency for Ethanol, Butanol and Propanol.

1.9 THz and 3 THz. The 1 THz loss in containment amounts to 5.75×10^{-08} dB/m for Ethanol, 6.11×10^{-08} dB/m for Butanol and 5.70×10^{-08} dB/m for Propanol.

For variations of ±3% with optimal design parameters, Fig. 8 displays the loss of containment vs frequency of the designed C-PCF. The figure shows that the loss of containment has declined because of the increase in frequency. In the frequency ranges from 1.9 THz to 3 THz, the containment loses are still constant.

The CL are 7.70×10^{-08}, 7.40×10^{-08} dB/m, and 7.35×10^{-08} dB/m for three alcohols such as ethanol, butanol and propanol to increment (+3%) for five layers diameter 293.55 μm respectively and the five coat pitches (individually) 391.40 μm, the core pitch of $A_c = 70.04$ μm and core diameter $d_c = 64.92$ μm. Besides, the CL are 7.30×10^{-08}, 7.50×10^{-08} dB/m, and 7.35×10^{-08} dB/m for three alcohols such as ethanol, butanol and propanol to decrement (−3%) for of 5 layers cladding diameter (individually) 276.45 μm and 5 layers cladding pitch (individually) 368.60 μm, 2 layers of core diameter (d_c) = 62.08 μm, core pitch (2 layers, A_c) = 65.96 μm.

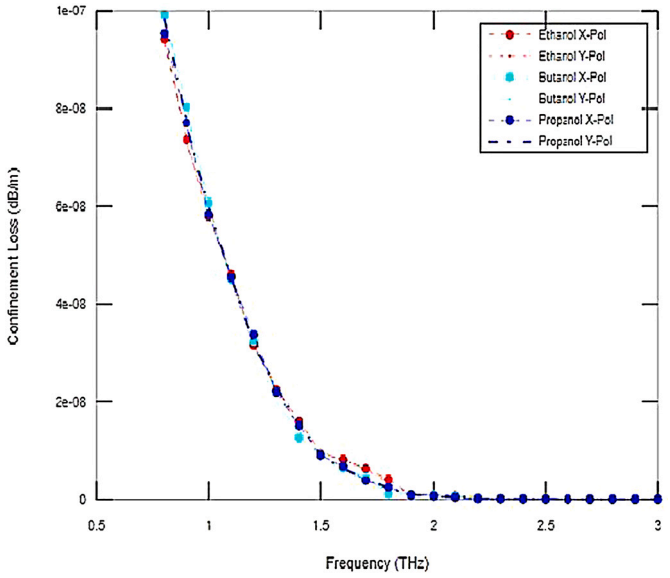

Fig. 7. CL of alcohol as a function of frequency for Ethanol, Butanol and Propanol.

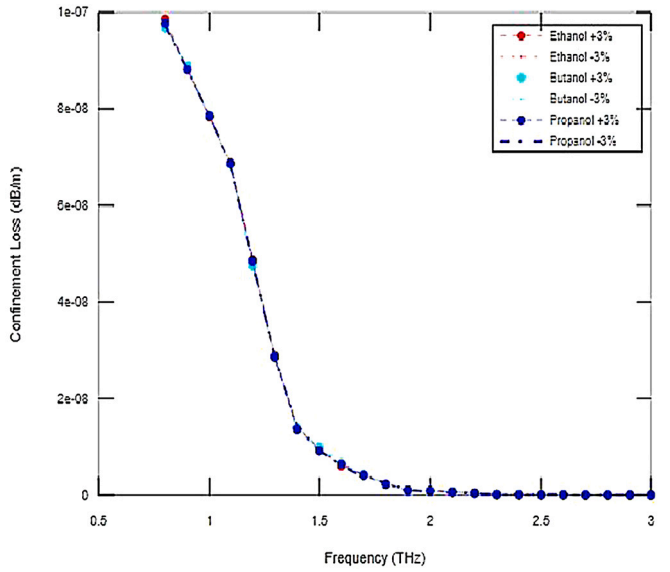

Fig. 8. CL of alcohol as a function of frequency for Ethanol, Butanol and Propanol at ±3% variations of core diameter.

Figs. 6 and 7 also show that the loss of containment vs frequency shows similar responses.

Fig. 9 shows the effective C-PCF fiber Index vs Frequency at the optimal x-polarization and y-polarization parameters. The figure indicates that in response to the increase in functional frequency the effective modus index is increasing. Effective mode Ethanol index values are 1.30, Butanol is 1.31 and Propanol 1.27 at 1 THz. The highest value of an effective mode index is also found for the specified alcohols substances (e.g., Ethanol, Butanol, and Propanol) at 3 THz which is 1.354, 1.3993 and 1.387.

Fig. 10 shows a 3% greater or less than that of the optimum parameters, the effective mode index vs. frequency curve for a designed C-PCF fiber. The figure shows that the effective mode index increases with the increase in the THz frequency. In the case of 3 EMIs, the core composition of Ethanol, Butanol and Propanol is 1.31, 1.32 and 1.30 for increment (+3%) parameters of parameters for five layers diameter

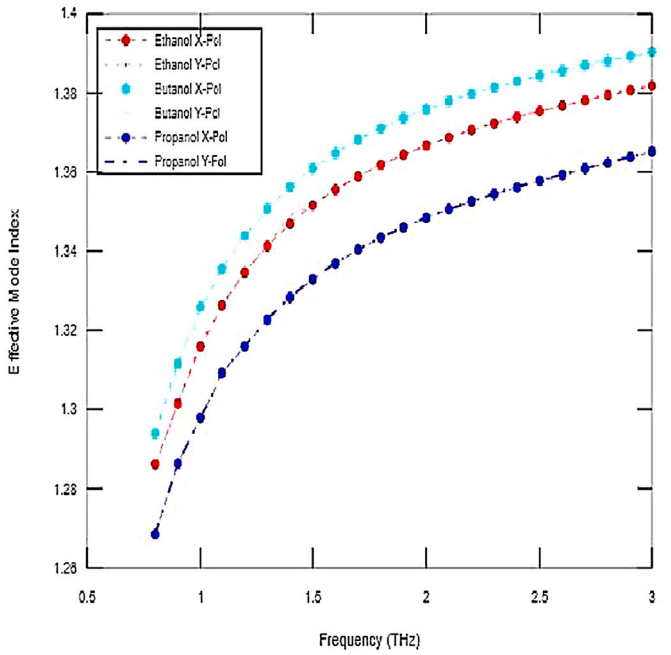

Fig. 9. Effective mode index as a function of frequency of for Ethanol, Butanol and Propanol at variable x and y.

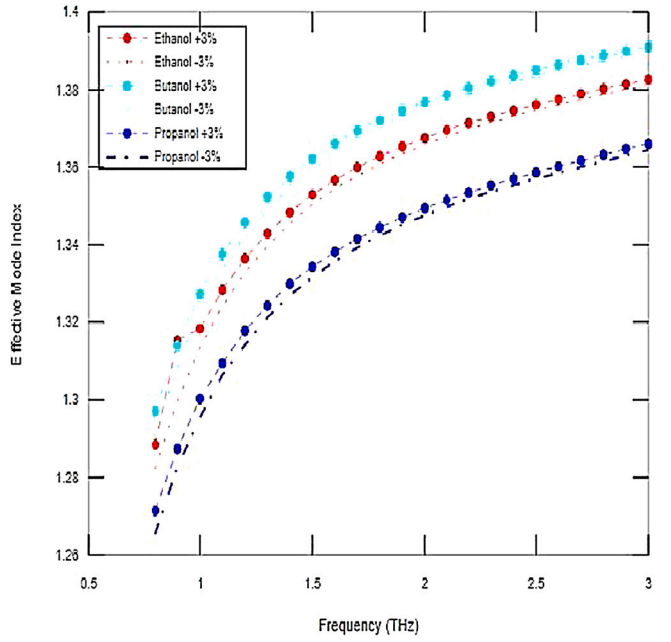

Fig. 10. Effective mode index as a function of frequency for Ethanol, Butanol and Propanol at ±3% variations of core diameter.

individually 293.55 μm and the five coat pitches of 391.40 μm, the core pitch of $A_c = 70.04$ μm and core diameter $d_c = 64.92$ μm along with the EMI are 1.30, 1.31 and 1.29 for 3 alcohols which are Ethanol, Butanol and Propanol at 1 THz for decrement (−3%) strictures of 5 layers cladding diameters individually 276.45 μm and 5 layers cladding pitch individually as 368.60 μm, 2 layers of core diameter (d_c) = 62.08 μm, core pitch (2 layers, A_c) = 65.96 μm.

From the above Fig. 9 and Fig. 10, we can conclude that the graphical behavior of the effective mode index vs frequency depicts similar output results in the THz wave.

Fig. 11 illustrates the overall power fraction of the proposed C-PCF

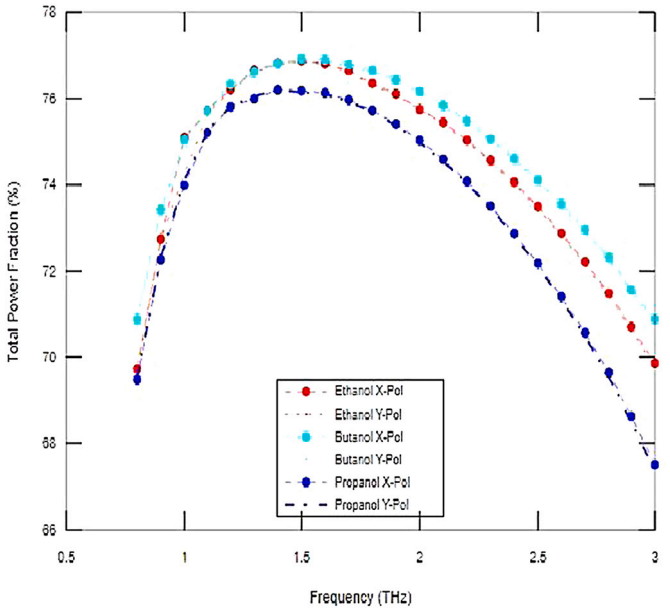

Fig. 11. Total power fraction as a function of frequency for Ethanol, Butanol and Propanol.

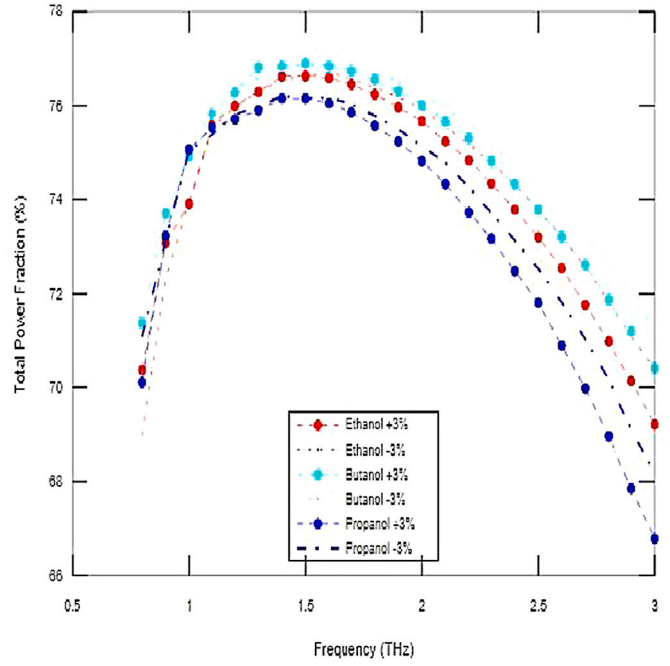

Fig. 12. Total power fraction as a function of frequency for Ethanol, Butanol and Propanol at ±3% variations of core diameter.

with optimal design parameters compared to the frequency of both polarizations. When the frequency range is extended, the overall power percentage increases from 0.80 THz to 1.50 THz. Then, the energy fraction falls from 1.50 THz to 3 THz. Here, there is an increasing total power fraction. We have found maximum power fraction is 78.10, 79.06 and 77.97 respectively for the three substances Ethanol, Butanol and Propanol in 1 THz frequency waveguide.

Fig. 12 shows the total power fraction versus the frequency of the planned C-PCF when the 3% or more changes are made than those of the ideal parameters. The value of the maximum power fraction has been increased in the frequency range 0.80 to 1.50 THz and the value of the maximum frequency wave of THz is reduced from 1.65 THz to 3 THz. The peak PF standards are 75.40, 76.30, 74.90 for 3 alcohols such as Ethanol, Butanol and Propanol. They are 1 THz in increase (+3%) parameters for five layers diameter individually 293.55 μm and the five coat pitches of individually 391.40 μm, the core pitch of $A_c = 70.04$ μm and core diameter $d_c = 64.92$ μm. Besides, 74.75, 75.55 and 73.35 are the peak values of power fraction at 1 THz for three alcohols such as Ethanol, Butanol and Propanol for decrement (−3%) strictures of 5 layers cladding diameters 276.45 μm respectively and 5 layers cladding pitch 368.60 μm, 2 layers of core diameter (d_c) = 62.08 μm, core pitch (2 layers, A_c) = 65.96 μm.

Finally, from Figs. 11 and 12, we find that the peak values are different but the power fraction versus frequency discloses similar graphical simulation outputs in the terahertz (THz) wave regions.

The ideal design and design of optical possibilities such as the RS and the CL of the C-PCF have also shown ±3% contrasts. Table 1 clearly shows a small sum of considerable differences between the ±3% variations, and the RS and CL are ideal for relaxation. We thus choose excellent plans to escape the complexity of the manufacture. Therefore, ready to say firmly that for reasons of location for chemicals, the proposed C-PCF structure within the industry or biomedicine regions is more reasonable.

The designed C-PCF shows a higher RS and a lower CL than other types of PCFs that is displayed in Table 1. The designed C-PCF based sensor indicates an improved method for detecting industrial and biomedical chemicals.

In response to Table 2, it is seen that the designed C-PCF will be more suitable for the application of chemical detections and identifications than the previously published reported articles [23–29].

The manufacturing technology is key to the design of the C-PCF structure based on the optical sensor. The different manufacturing processes of PCF are presented today, including stacking, jacketing, collapsing and stretching on a conventional drawing tower. In recent times, however, the sol-gel [30] process for the manufacture of the PCF structure with optical sensors is most commonly used and is better suited for the manufacture of the PCF structure based on sensors. In addition, the selective filling technique [31] is better suited for filling or loading chemical products into the core areas with any PCF fiber structure. Thus, by applying the latest technology production process for filling up technique fabrication process, we achieved better guiding properties like effective area, RS, power fraction, CL, and effective mode index.

5. Conclusion

Humans are extremely vulnerable to the effects of alcoholic agents. Given the amount of danger, an effective and adaptable alcohol detection technology is critical. In this context, a hollow core photonic crystal fiber (HC-PCF)-based optical sensor with circular air holes in the cladding section and a hexahedron core is proposed for detecting alcohol in drinks as well as other liquid samples. COMSOL Multiphysics software with a finite element technique as a solver is used to develop and analyze the sensing properties of a PCF-based sensor. In the THz frequency band, the described PCF structure has an exceptionally high sensitivity of 86.60%, 88.70%, and 84.71% and low confinement losses are 5.75×10^{-08}, 6.11×10^{-08} dB/m and 5.70×10^{-08} dB/m Ethanol ($n = 1.354$), Butanol ($n = 1.399$), and Propanol ($n = 1.387$), respectively at monitoring region of 1 THz. So, we know that an alcohol is widely utilized in both chemical industrial processes and the food and beverage industries. As a result, we can say clearly that the alcohols detection system-based C-PCF in the terahertz frequency range will be perfect for alcohols detection with successfully.

Funding statement

The authors have not received any funding for this research.

Table 1
Comparison along with the ±3% differences and the optimal possessions at the area of 1 THz.

Parameters (%)	RS (%)			CL (dB/m)		
	Ethanol	Butanol	Propanol	Ethanol	Butanol	Propanol
+3%	87.20%	89.40%,	85.30%	7.70×10^{-08}	7.40×10^{-08}	7.35×10^{-08}
Optimum	86.60%	88.70%,	84.71%	5.75×10^{-08}	6.11×10^{-08}	5.70×10^{-08}
−3%	85.10%,	87.30%	83.15%	7.30×10^{-08}	7.50×10^{-08}	7.35×10^{-08}

Table 2
Comparison between C-PCF and previously designed different PCF structure in response to RS and CL.

Prior in PCFs	Operating region (f) THz	RS (%)	CL (dB/m)	Design of structure	
				Core	Cladding
PCF_1 [23]	1	60.05	1.43×10^{-11}	Rotated-Hexa circular holes	Heptagonal
PCF_1 [24]	1	64.00	1.12×10^{-11}	Elliptical holes	Quasi
PCF_1 [25]	1	74.54	7.72×10^{-08}	Slotted core	Quasi
PCF_1 [26]	1	78.80	2.19×10^{-09}	Elliptical holes	Quasi
PCF_1 [27]	1	45.13	5.583×10^{-05}	Circular holes	Hexagonal
PCF_1 [28]	1	55.56	1.00	Rhombic holes	Hexagonal
PCF_1 [29]	1	80.93	1.23×10^{-11}	Elliptical hole	Circular
Proposed	1	86.60	5.40×10^{-08}	Hexahedron	Circular

Author contributions

All authors are equally contributed of this research work.

Availability of data and material

This paper has sufficient data which has been taken from COMSOL Multiphysics software by simulation the work.

Code availability

This paper has sufficient code or graph which has been taken from COSMOL Multiphysics software and then plotted by MATLAB software.

Compliance with ethical standards

No bad ethical value has been included in this paper.

Consent to participate

All authors are agreed to submit the paper in this journal.

Consent for publication

All authors are agreed to publish the paper in this journal.

Ethics approval

No unethical work has been performed in this research work.

Declaration of Competing Interest

The authors declare that they have no competing of interest.

Acknowledgements

The authors are grateful to the participants who contributed to this research. The authors have not received any funding for this research.

References

[1] M.R. Hasan, M.S. Anower, M.A. Islam, S.M.A. Razzak, Polarization-maintaining low-loss porous core spiral photonic crystal fiber for terahertz wave, Appl. Optics 55 (15) (2016).
[2] K. Kawase, Y. Ogawa, Y. Watanabe, H. Inoue, Non-destructive terahertz imaging of illicit drug using spectral fingerprint, Optical Exp. 11 (2003) 2549–2554.
[3] C.J. Strachan, P.F. Taday, D.A. Newnham, K.C. Gordon, J.A. Zeitler, M. Pepper, T. Rades, Using terahertz pulsed spectroscopy to quantify pharmaceutical polymorphism and crystallinity, J. Pharm. Sci. 94 (2005) 837–846.
[4] A.y. Pawar, D.D. Sonawane, K.B. Erande, Terahertz technology and its applications, Drug Invent. Today (2013) 157–163.
[5] F. Iqbal, S. Biswas, A.A.-M. Bulbul, H. Rahaman, Md.B. Hossain, Md.E. Rahaman, Md.A. Awal, Alcohol sensing and classification using PCF-based sensor, Sensing Bio-Sens. Res. 30 (2020) 100384. ISSN 2214-1804, https://doi.org/10.1016/j.sbsr.2020.100384.
[6] A.A.-M. Bulbul, A.Z. Kouzani, M.A.P. Mahmud, A.-A. Nahid, Design and numerical analysis of a novel rectangular PCF (R-PCF)-based biochemical sensor (BCS) in the THz regime, Int. J. Optics 2021 (2021), https://doi.org/10.1155/2021/5527724. Article ID 5527724, 16 pages.
[7] A.A.-M. Bulbul, A.N.Z. Rashed, H.M. El-Hageen, A.M. Alatwi, Design and numerical analysis of an extremely sensitive PCF-based sensor for detecting kerosene adulteration in petrol and diesel, Alexandr. Eng. J. 60 (6) (2021) 5419–5430. ISSN 1110-0168, https://doi.org/10.1016/j.aej.2021.04.041.
[8] Shuvo S., Shafi M.A, Sikder A.S., Hossain Md. S., Azad M.M., "Zeonex based decagonal photonic crystal fiber (D-PCF) in the terahertz (THz) band for chemical sensing applications", Sensing Bio-Sens. Res. https://doi.org/10.1016/j.sbsr.2020.100393(2020).
[9] S. Nivedha, K. Senthilnathan, Design of a terahertz alcohol sensor using a steering-wheel microstructured photonic crystal fiber, IETE J. Res. (2020), https://doi.org/10.1080/03772063.2020.1808535.
[10] M.S. Hossain, S. Sen, M.M. Hossain, Performance analysis of octagonal photonic crystal fiber (O-PCF) for various communication applications, Phys. Scr. 96 (5) (2021) 55506, https://doi.org/10.1088/1402-4896/abe323.
[11] M.F.H. Arif, K. Ahmed, S. Asaduzzaman, M.A.K. Azad, Design and optimization of photonic crystal fiber for liquid sensing applications, Photon. Sens. 6 (2016) 279–288.
[12] J. Sultana, M. Islam, K. Ahmed, A. Dinovitser, W.-H.N.G. Brian, D. Abbott, Terahertz detection of alcohol using a photonic crystal fiber sensor, Appl. Opt. 57 (10) (2018) 1.
[13] B.K. Paul, K. Ahmed, S. Asaduzzaman, M.S. Islam, Folded cladding porous shaped photonic crystal fiber with high sensitivity in optical sensing applications: design and analysis, Sensing Biosens. Res. 12 (2017).
[14] H. Ademgil, S. Haxha, PCF based sensor with high sensitivity, high birefringence and low CLes for liquid analyte sensing applications, Sensors, MDPI (2015) 31833–31842.
[15] K. Ahmen, B.K. Paul, S. Chowdhury, S. Sen, M.I. Islam, M.S. Islam, M.R. Hasan, S. Asaduzzaman, Design of a single mode photonic crystal fiber with ultra-low material loss and large effective mode area in THz regime, IET Optoelect. 11 (6) (2017) 265–271.
[16] A.M. Cubillas, S. Unterkofler, T.G. Euser, B.J.M. Etzold, A.C. Jones, P.J. Sadler, P. Wasserscheid, P. St, J. Russell, Photonic crystal fibres for chemical sensing and photochemistry, Chem. Soc. Rev. 42 (22) (2013) 8629–8648.
[17] F.H. Arif, K. Ahmed, S. Asaduzzaman, A.K. Azad, Design and optimization of photonic crystal fiber for liquid sensing applications, Photon. Sensors 6 (3) (2016) 279–288.
[18] K. Ahmed, F. Ahmed, S. Roy, et al., Refractive index-based blood components sensing in terahertz spectrum, IEEE Sensors J. 19 (9) (2019) 3368–3375.
[19] Md. Abdullah-Al-Shafi, N. Akter, Md. Shuvo Sen, S. Hossain, Design and performance analysis of background material of zeonex based high core power fraction and extremely low effective material loss of photonic crystal fiber in the terahertz (THz) wave pulse for many types of communication areas, Optik 243 (2021) 167519. ISSN 0030-4026, https://doi.org/10.1016/j.ijleo.2021.167519.
[20] Md.S. Islam, J. Sultana, J. Atai, M.R. Islam, D. Abbott, Design and characterization of a low-loss, dispersion-flattened photonic crystal fiber for terahertz wave propagation, Optik – Int. J. Light Electron Optics. 145 (2017) 398–406.

[21] H. Ademgil, S. Haxha, Highly PCF based sensor with high sensitivity, high birefringence and low confinement losses for liquid analyte sensing applications, Sensors 15 (12) (2015) 31833–31842.
[22] Md.F.H. Arif, K. Ahmed, S. Asaduzzaman, Md.A.K. Azad, Design and optimization of photonic crystal fiber for liquid sensing applications, Photon. Sensors 6 (3) (2016) 279–288.
[23] M.R. Hasan, M.A. Islam, A.A. Rifat, A single mode porous-core square lattice photonic crystal fiber for THz wave propagation, J. Eur. Opt. Soc. Rapid Publ. 12 (1) (2016) 15, https://doi.org/10.1186/s41476-016-0017-5.
[24] K. Ahmed, S. Chowdhury, B.K. Paul, M.S. Islam, S. Sen, M.I. Islam, Ultrahigh birefringence, ultralow material loss porous core single-mode fiber for terahertz wave guidance, Appl. Opt. 56 (12) (2017) 3477–3483, https://doi.org/10.1364/AO.56.003477.
[25] S. Rana, G.K. Hasanuzzaman, S. Habib, S.F. Kaijage, R. Islam, Proposal for a low loss porous core octagonal photonic crystal fiber for T-ray wave guiding, Opt. Eng. 53 (11) (2014) 115107, https://doi.org/10.1117/1.OE.53.11.115107.
[26] Md Saiful Islam, J. Sultana, K. Ahmed, M. Rakibul Islam, A. Dinovitser, B. Wai-Him Ng, D. Abbott, A novel approach for spectroscopic chemical identification using photonic crystal fiber in the terahertz regime, IEEE Sensors J. 18 (2018) 575–582.
[27] Md Saiful Islam, J. Sultana, A.A. Rifat, A. Dinovitser, B. Wai-Him Ng, D. Abbott, Terahertz sensing in a hollow core photonic crystal fiber, IEEE Sensors J. 18 (2018) 4073–4080.
[28] M.R. Hasan, M.A. Islam, M.S. Anower, S.M. Razzak, Low-loss and bend-insensitive terahertz fiber using a rhombic-shaped core, Appl. Opt. 55 (30) (2016) 8441–8447, https://doi.org/10.1364/AO.55.008441.
[29] G.K.M. Hasanuzzaman, S. Rana, M.S. Habib, A novel low loss, highly birefringent photonic crystal Fiber in THz regime, IEEE Photon. Technol. Lett. 28 (April 8) (2016) 899–902.
[30] H. El Hamzaoui, Y. Ouerdane, L. Bigot, G. Bouwmans, B. Capoen, A. Boukenter, S. Girard, M. Bouazaoui, Sol-gel derived ionic copper-doped microstructure optical fiber: a potential selective ultraviolet radiation dosimeter, Opt. Express 20 (28) (2012) 29751–29760.
[31] M.S. Hossain, S. Shuvo, M.M. Hossain, Design of a chemical sensing circular photonic crystal fiber with high RS and low CL for terahertz (THz) regime, Optik – Int. J. Light Electron Optics 222 (2020), 165359, https://doi.org/10.1016/j.ijleo.2020.165359(2020).